Available online at www.sciencedirect.com
ScienceDirect
Physica C 468 (2008) 832–836
PHYSICA C
www.elsevier.com/locate/physc

Vortex imaging with varying temperature revealed by SHPM on $Bi_2Sr_2CaCu_2O_{8+y}$

V. Mihalache [a,*], M. Dede [b], A. Oral [b], V. Sandu [a]

[a] National Institute of Materials Physics, P.O. Box MG-7, Bucharest-Magurele 077125, Romania
[b] Bilkent University, Ankara, Turkey

Accepted 30 November 2007
Available online 29 February 2008

Abstract

Scanning Hall probe microscopy with an effective spatial resolution of ~1 μm has been used to investigate the vortex structures in superconducting $Bi_2Sr_2CaCu_2O_{8+\delta}$ single crystals in the temperature range 77.3–81.3 K and zero applied field (in the presence of the earth field). The vortex images were obtained in real time mode as the temperature increased slowly for 3.36 h. At 77.3 K, the vortices were arranged in a chain structure. With the increase of the temperature, two jumps in the vortex array occur at 77.3 K, immediately when the temperature starts to rise, and at 79.2 K with a good stability between jumps. The second jump is accompanied by the jump in the average magnetic induction when bundles of 4–5 additional vortices enter the scanning area and the vortex array get disordered. These directly visualized transitions in the vortex lattice are consistent with a vortex creep over the surface barriers at high temperatures. A short movie is presented.

PACS: 74.72.Hs; 74.25.Ha; 74.25.Op; 74.25.Qt

Keywords: Vortex imaging; Vortex structure; Bi-2212; Surface barriers

1. Introduction

Investigation of flux structures and dynamics of the dilute vortex lattice, are useful for the optimization and improving the performances of the devices based on the motion of the single flux quanta.

For very small fields, $B \ll \Phi_0/\lambda^2$ (where $\Phi_0 = 2.07 \times 10^{-7}$ G cm^2 is the flux quantum and λ the magnetic field penetration length), the vortices are well separated, their interaction is week, and only the nearest neighbors vortices substantially contribute to the interaction energy of the system [1].

Usually, data on the structure and dynamics are obtained from either macroscopic measurements or microscopic probes whose signal is the average of a large ensemble of vortices. For the better understanding the physical phenomenon, in particularly that observed at macroscopic level in layered superconductors it is important to extend these studies to the truly microscopic (local) level.

In order to register the motion of individual vortes, Geim et al. [2] used a method based on the measurements of the vortex-induced magnetoresistance in a normal-metal microprobe. The direct imaging of the vortex lattice were carried out on stabilized (relaxed) lattices for a given flux and temperature. There are few exceptions like the direct observation of melting of the vortex solid in $Bi_2Sr_2CaCu_2O_{8+\delta}$ (Bi-2212) single crystals by Oral et al. [3]. An interesting example of direct visualization of the vortex dynamics in Bi-2212 crystal at 77.3 K, when the applied field increases, is given in the Ref. [4]. Nevertheless, no direct visualization of the vortex dynamics with varying temperature was carried out to our knowledge.

* Corresponding author.
E-mail address: vmihal@infim.ro (V. Mihalache).

0921-4534/$ - see front matter © 2008 Elsevier B.V. All rights reserved.
doi:10.1016/j.physc.2007.11.059

We report here the first direct observations on the vortex dynamics in diluted flux line lattice with increasing temperature in Bi-2212 single crystals using a scanning Hall probe microscope (SHPM) with an outstanding field sensitivity of $\sim 3 \times 10^{-7}$ THz$^{-1/2}$ and a spatial resolution ~ 1 μm.

2. Experimental

The design of low temperature scanning Hall Probe Microscope (LT-SHPM) used in this work is presented in detail elsewhere [5]. The active Hall sensor has an effective spatial resolution of ~ 1 μm, and a scan area of about $\sim 13 \times 13$ μm^2. The measurements were performed in narrow temperature range 77.3–81.3 K in the very weak earth magnetic field (residual field near the scanner head).

To avoid the excess of temperature fluctuation the heater was switched off and the increase of the temperature was achieved by closing the needle valve in the cryostat device.

We used high quality as-grown Bi-2212 single crystals with the area of the *ab* plane of 2×2.5 mm^2 and a thickness of about 100 μm. The critical temperature of the samples was 84.7 K, as determined from $H_p(T)$ (or $H_{c1}(T)$) curve.

SHPM measurements were performed after earth-field-cooling (EFC) of the crystals down to 77.3 K and the processes were shot in a movie consisting of 133 images.

3. Results

By cooling the Bi-2212 single crystal in low applied fields, a residual induction of order of few tenths of Oersteds remains trapped within the sample and the vortices stabilize in chains. Examples of such assembly of vortices are shown in the Fig. 1. The reason of this chain-like arrangement at very low field in the absence of a component of the applied field parallel to the ab plane is still under debate.

Fig. 2 shows nine SHPM scans at different temperatures, chosen from the 133 images of the attached movie. The time variation of the temperature is shown in the Fig. 3 with a zoomed in of the initial instant when the temperature starts rising shown in the inset. Each picture in Fig. 2 (movie) corresponds to only one scan taken in real time scanning mode (~ 1 frame/s) and not to an average on several images. One can exactly evaluate the average

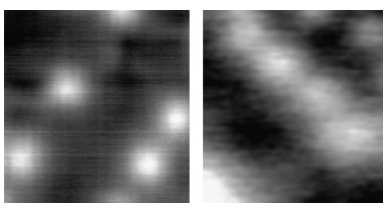

Fig. 1. SHPM images after earth-field-cooling (EFC) to 77.3 K taken on two Bi-2212 single crystals of the same quality as the crystal studied in this paper (image (a) is taken from Ref. [4]). The stable vortex lattice consists of flux lines arranged in the line. Scan size is 13×13 μm^2.

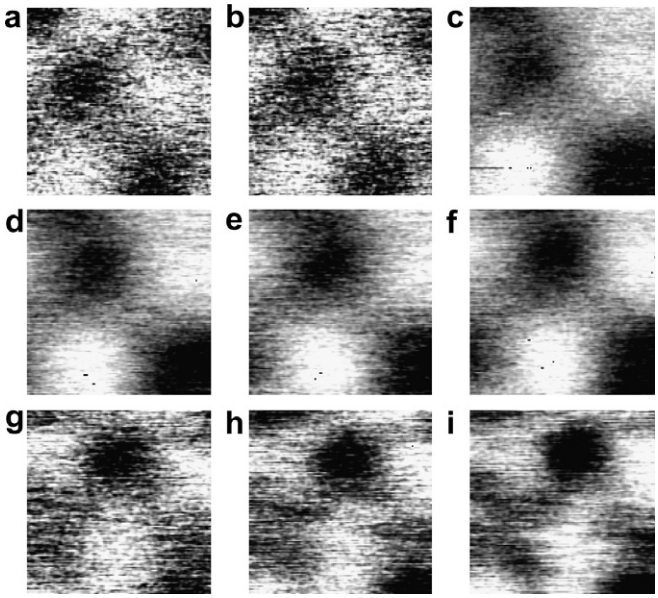

Fig. 2. SHPM images obtained in real time scanning mode during the temperature increase from 77.3 K to 81.3 K: (a) image 5, $T = 77.3$ K, $t = 1273$ s; (b) image 18, $T = 77.301$ K, $t = 4036.74$ s; (c) image 19, $T = 77.303$ K, $t = 4217.35$ s; (d) image 50, $T = 77.53$ K, $t = 6726.2.19$ s; (e) image 55, $T = 77.78$ K, $t = 7458.7$ s; (f) image 59, $T = 78.17$ K, $t = 8533$ s; (g) image 89, $T = 79.15$ K, $t = 10308.3$ s; (h) image 90, $T = 79.2$ K, $t = 10348$ s; (i) image 133, $T = 81.3$ K, $t = 12099$ s. The images are reversed. Scan size is 13×13 μm^2. Attached movie presents 133 images.

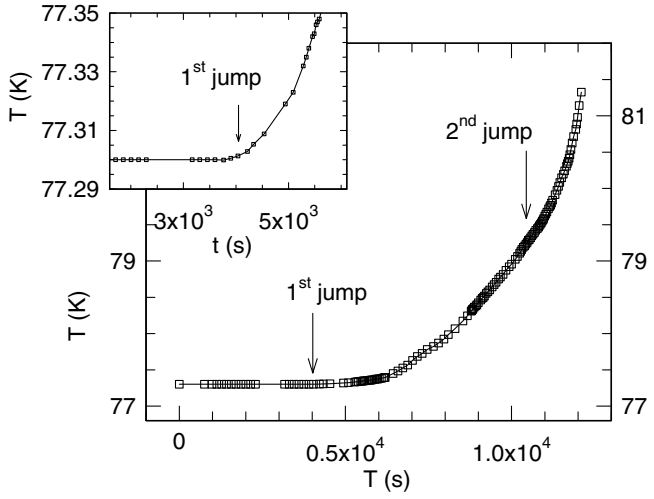

Fig. 3. Time t dependence of the temperature T during the experiment. Two arrows indicate t and T at which two jumps (Fig. 2b–c and f–g) in the vortex configuration occur. Inset: zoom in of the same plot close to the first jump occurring when the temperature starts to rise.

magnetic induction from the number N of vortices present in the scanned area a^2 as

$$\langle B \rangle = N \frac{\Phi_0}{a^2}, \tag{1}$$

As can be seen in Fig. 2 for the constant temperature, the configuration of the vortex lattice is stable, Fig. 2a (image 5) and b (image 18). The vortices are arranged in the line,

hence, the total number of vortices is $N \approx 3$ and the average induction calculated using Eq. (1) is $\langle B \rangle \approx 0.34$ G. Actually, this is the residual field generated by the applied (earth) field as will be seen clearly below.

The first jump in the vortex configuration (Fig. 2c (image 19)) occurs when the temperature starts to increase as can be seen in the inset to Fig. 3. After the jump, two single-flux vortices in the right-up corner tend to form a bundle whereas the vortex from the bottom joins into another bundle. Note that the average induction did not change in this process.

A further increase of the temperature from 77.3 K up to 79.2 K leads to a clear tendency of motion of the entire ensemble of vortices towards right-up corner, though its configuration and the magnetic inductions do not change (Fig. 2c–f). A proof of this motion is that the right-up vortex vanishes from the scanned area in the image 18 (Fig. 2b) and another vortex (or bundle) enters the left-down corner in the image of Fig. 2e (image 55) and f (image 59); particularly, the first jump was accompanied by a similar displacement of the vortex lattice (compare the images of Fig. 2b and c).

The second jump in the vortex configuration, which occurs at 79.2 K (image 89 in Fig. 2g), involves a jump in the number of vortices (magnetic induction) as well. The average induction after the second jump is $\langle B \rangle \approx 0.9$ G. The most important fact is that the flux entered (hopped) the scanned area as bundles consisting of 4–5 vortices. Between the image 89 in Fig. 2g and the image 133 in Fig. 2i the configuration of vortex lattice and the number of vortices (magnetic induction) did not change significantly even though the temperature was raised by 2 K.

4. Discussion

The noticeable flux-creep towards right-up corner direction even in the frame of the same vortex configuration (images c–f and g–i in Fig. 2) indicates the action of some energetically barriers. A significant bulk pinning is unlikely at the elevated temperatures where the investigations were carried out in Bi-2212. Indeed, it was shown that, at high temperatures, bulk pinning is very weak and the hysteresis loop, hence, the irreversibility, is mainly due to the surface and geometrical barriers [6]. No significant vortex creep over the geometrical barriers was detected within the experimental time scale 10^{-5}–10^{-1} Oe/s on Bi-2212 [7]. To date, both the theoretical reports and experimental data indicate that the vortex creep over surface barriers in "clean" layered superconductors like Bi-2212 prevails over any other barrier at elevated temperatures.

A typical local magnetization curve taken at 77.3 K on our single crystal is shown Fig. 4. Since the induction B inside the sample was measured directly by the Hall probe, the magnetization is defined as the difference between induction and the applied field, $M = B - H$. A hint of the existence of the surface barriers is the asymmetric shape of the hysteresis loop, *i.e.*, a sharp drop-off in magnetization above flux penetration on the ascending (increasing absolute value of the field) branch, and the nearly flatness of the descending (decreasing absolute value of the field) branch. Additionally, the absence of any change of the sign of the magnetization on the descending branch suggests the absence of the bulk pinning. Therefore, the dynamics of vortices should be determined mainly by the elastic energy of the flux line lattice (vortex–vortex interaction) and the presence of the surface barriers in this temperature range.

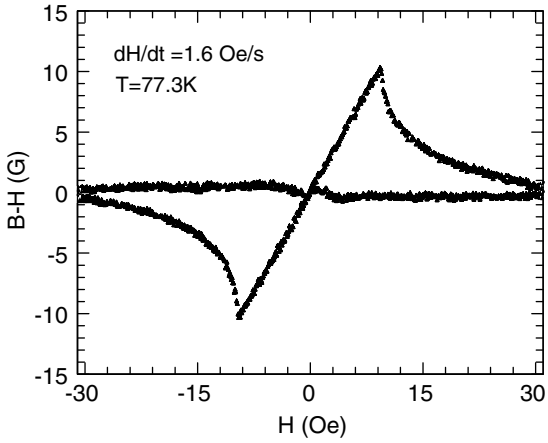

Fig. 4. Local magnetization loop measured at 77.3 K and a sweep rate of 1.6 Oe/s.

First, we discuss the second jump in the vortex configuration at 79.2 K after that the induction rise with almost 0.7 G.

In the absence of surface barriers the flux enters (exits) the sample at first penetration field H_{c1} [1,8],

$$H_{c1} = \frac{\Phi_0}{4\pi\lambda^2} \ln\frac{\lambda}{\xi}, \tag{2}$$

at which the internal flux tread becomes energetically favourable. The presence of the surface effects prevents the flux entering at H_{c1} until a higher thermodynamic critical field H_c is reached. In the real samples, the first flux entering occurs at full flux penetration field H_p, which lies somewhere in between: $H_{c1} < H_p < H_c$ [9].

In HTSC, at higher temperatures, the field at H_p is predicted to enter by the creep of the vortex half-loops over the surface barriers as [10]

$$H_p \propto (T_c - T)^{3/2}/T \tag{3}$$

As the temperature increases, the system should cross the $H_p(T)$ line described by Eq. (3). Only in the case of a degraded surface, the system crosses $H_{c1}(T)$ line when T increases. Fig. 5 shows two $H_p(T)$ curves taken at two different sweep rates, 39.2 Oe/s and 6.5 Oe/s, obtained from the peak fields of isothermal magnetization curves similar to that shown in Fig. 4. For decreasing dH/dt, the surface barriers decrease (see [7]), and vanish at zero rate. Therefore, the lower critical field was defined as $H_{c1}(T) = H_p(T, dH/dt \to 0)$ in the same figure. The lowest

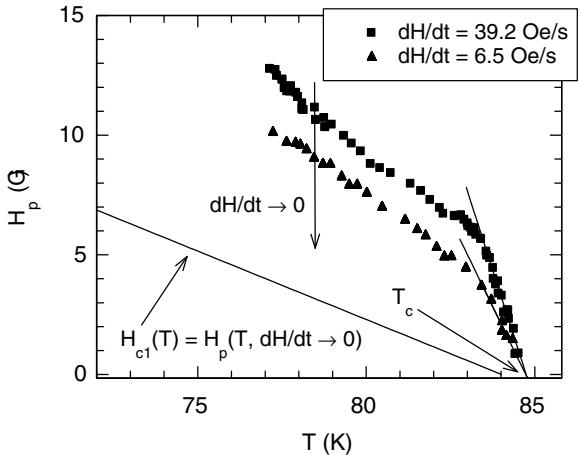

Fig. 5. Temperature T dependence of the first penetration field H_p measured at sweep rates of 39.2 Oe/s and 6.5 Oe/s. The lower critical field is defined as $H_{c1}(T) = H_p\,(T,\, dH/dt \to 0)$.

rate we have used was $dH/dt = 10^{-2}$ Oe/s. The details of this subject will be reported elsewhere.

The data shown in Fig. 5 gives $H_{c1} \approx 3.8$ G at 77.3 K, a value well above $\langle B\rangle \approx 0.34$ G that suggests a highly diluted residual vortex lattice. At 79.2 K, where the second jump occurs, $H_{c1} \approx 2.8$ G is again above the experimentally calculated induction $\langle B\rangle \approx 1.1$ G. Accordingly to the same $H_{c1}(T)$ line, the penetration of the field of 1.1 G into the sample would occur at ~81.3 K. However, the curves in Fig. 5 were not subjected to corrections for the demagnetizing factor. The field near the surface of the rectangular sample with the thickness d, and the smaller transverse size w in the Meissner state is $(w/d)^{1/2}$ times larger than the applied field, thus the penetration field is $(d/w)^{1/2}H_p$ [10,11]. Therefore, the field penetrates at a lower temperature, namely at 79.2 K instead 81.3 K. In this way, the evolution of the Bi-2212 system (dynamics of diluted vortex lattice) with varying temperature attends the following scenario as observed in vortex imaging. The crystal was submitted to an EFC at $H_{earth} = H_a \approx 1.1$ G from a temperature above the critical one $T_c = 84.7$ K down to 77.3 K. At $T \approx 79.2$ K, when H_a (or $\langle B\rangle$) $= H_p \approx H_{c1}$, the field leaves the sample (though a residual field of $H_{residual} = \langle B\rangle \approx 0.34$ G still survives). Our experimental route of vortex imaging follows an opposite direction. The temperature starts to rise from $T = 77.3$ K in the presence of the residual field $H_{residual}$. As temperature increases, the surface barriers for the flux creep should decrease (see Fig. 5). At 79.2 K, the system crosses $H_p(T) \approx H_{c1}$ line at which the thermal activation over surface barrier occurs via the creation and further expansion of the half-loop excitations [9,10,12]. The fast increase of $\langle B\rangle$ towards the higher expected value $H_a = 1.1$ Oe, at this temperature (Fig. 3a) is attributed to the rapid flux entry caused by the decrease of the surface energy barrier. Indeed, Fig. 2j–i, show that a further T increase up to 81.3 K does not induce noteworthy changes in flux line configuration and in the magnetic induction. This suggests, in particularly, that above 79.2 K the difference between $\langle B\rangle$ and H_a is small and no significant number of vortices enter the sample anymore.

The simultaneous appearance of 4–5 vortices within the scanned area (hopping bundles) is in good agreement with theoretical predictions of Burlachkov et al. [10] who have shown that vortices penetrate through the surface via creation of critical nuclei consisting of several vortex lines [12]. The process was experimentally evidenced in vortex-induced magnetoresistance [2].

As regarding the first jump in the vortex lattice configuration at 77.3 K, this is, in our opinion, the result of the highly diluted vortex lattice. In such a system the vortices are extremely separated, the interaction between them is exponentially weak and the vortex structure is very soft. It seems that the beginning of the temperature increase together with the action of the surface barriers on such a diluted lattice create a tension in it which relaxes at some critical value in the form of vortex bundles. The evidence of the permanent action of "surface pressure" is given by the tendency of the motion of the entering vortex structure towards the sample center (towards the right-up corner) in the frame of the same vortex configuration (images b–f and g–i in Fig. 2). The same dilution of the vortex lattice hinders its relaxation in the Abrikosov state above H_{c1}(see images in Fig. 2g–i). Both single-flux vortices and vortex bundles form the vortex lattice in this region of H–T diagram.

5. Conclusions

We report the first direct observation of the vortex dynamics in the diluted vortex lattice with increasing temperature (from 77.3 K to 81.3 K) in Bi2212 single crystals using a scanning Hall probe microscope (SHPM). Two jumps in the vortex configuration were observed, the tendency of the motion of the entering vortex structure towards a direction (the sample center) even in the frame of the same vortices configuration where the magnetic induction is not changed, and the simultaneous penetration of a vortex bundle in the scanned area. During the temperature increase both single-flux vortices and vortex bundles form the vortex lattice in this region of the H–T diagram. The observed phenomena are in agreement with the theoretical predicted magnetic flux creep over surface barriers at high temperatures.

Acknowledgements

This work was supported by the Romanian NASR under the Project CEEX 21/2006 and the Scientific and Technical Research Council of Turkey (TUBITAK): Scientific Human Resources Development (BAYG) under the NATO PC Fellowships Program. Authors are grateful to K. Kadowaki and H. Shtrikman for their support and valuable advice.

References

[1] G. Blatter et al., Rev. Mod. Phys. 66 (1994) 1125.
[2] A.K. Geim et al., Phys. Rev. B 46 (1992) 324.
[3] A. Oral et al., Phys. Rev. Lett. 80 (1998) 3610.
[4] M. Dede et al., Jpn. J. Appl. Phys. 45/3B (2006) 2246.
[5] A. Oral, S.J. Bending, Appl. Phys. Lett. 69 (1996) 1324.
[6] D.D. Majer et al., Phys. Rev. Lett. 75 (1995) 1166.
[7] M. Nideröst et al., Phys. Rev. B 81 (1998) 3231.
[8] C.P. Bean, J.D. Livingston, Phys. Rev. Lett. 12 (1964) 14.
[9] L. Burlachkov, Phys. Rev. B 47 (1993) 8056.
[10] L. Burlachkov et al., Phys. Rev. B 50 (1994) 16 770.
[11] E. Zeldov et al., Phys. Rev. Lett. 73 (1994) 1428.
[12] A.E. Koshelev, Physica C 191 (1992) 219.